

Like-sign dilepton signature for gluino production at the CERN LHC including top quark and Higgs boson effects

Manoranjan Guchait

Physics Department, Jadavpur University, Calcutta 700 0032, India

D.P. Roy*

Theoretical Physics Group, Tata Institute of Fundamental Research, Bombay 400 005, India

(Received 19 December 1994)

A systematic analysis of the like-sign dilepton signature for gluino production at the CERN LHC is performed in the R -conserving minimal supersymmetric standard model, taking into account the top quark and Higgs boson effects in the cascade decay. We consider two representative values of the gluino mass, 300 and 800 GeV, along with those of the other SUSY parameters. While the top quark contribution is kinematically suppressed for the former case, it is very important for the latter. Ways of separating the signal from the background are discussed. One expects a viable like-sign dilepton signal up to a gluino mass of ~ 800 (1200) GeV at the low (high) luminosity option of the LHC over practically the full parameter space of the MSSM.

PACS number(s): 14.80.Ly, 12.60.Jv, 13.85.Qk, 13.85.Rm

I. INTRODUCTION

The CERN Large Hadron Collider (LHC) offers the possibility of squark \tilde{q} and gluino \tilde{g} searches right up to the predicted mass limit of ~ 1 TeV [1]. The canonical search strategy for these superparticles is based on the missing- p_T signature, which follows from R -parity conservation [2]. The latter implies that the superparticles are produced in pairs and the lightest superparticle (LSP) resulting from their decay is stable. It is also required to be colorless and neutral for cosmological reasons [3]. In most supersymmetric (SUSY) models of current interest it is the lightest neutralino χ_1^0 . The LSP is expected to escape detection due to its weak interaction with matter very much like the neutrino. The apparent imbalance of the transverse momentum resulting from this constitutes the missing- p_T signature for superparticle production.

There has been a growing realization in recent years, however, that an isolated multilepton and in particular a like-sign dilepton (LSD) signature may play an equally important role in superparticle searches [4–8]. For the R -conserving SUSY model of present interest, the main source of leptons in the \tilde{q} and \tilde{g} searches at the LHC is their cascade decay into the LSP. They proceed via the heavier chargino (neutralino) states by emission of a real or virtual $W(Z)$ boson, which has a significant leptonic branching fraction: e.g.,

$$\tilde{g} \rightarrow \bar{q}q'\chi_i^+, \quad \chi_i^+ \rightarrow W^+\chi_1^0 \xrightarrow{0.22} \ell^+\nu\chi_1^0, \quad (1)$$

$$\tilde{g} \rightarrow \bar{q}q\chi_i^0, \quad \chi_i^0 \rightarrow Z\chi_1^0 \xrightarrow{0.06} \ell^+\ell^-\chi_1^0, \quad (2)$$

where ℓ stands for both e and μ .

Recently a systematic analysis of the isolated LSD sig-

nature for gluino pair production at the LHC was undertaken in [9] for both R -conserving and R -violating SUSY models. In the R -conserving model, the dilepton final state of interest arises mainly from the cascade decay (1) of both the gluinos. After putting in the leptonic branching fractions of both the W bosons one gets an overall branching fraction of $\sim 1\%$ for the decay of the gluino pair into a dilepton final state. Half of these are expected to be LSD's since the gluino is a Majorana particle. Despite the small branching fraction the isolated LSD signature was shown to be viable for gluino searches at the LHC because of the small background in this channel [9]. The main source of background is $t\bar{t}$ production. There is a LSD background from the direct leptonic decay of one t while the other decays into a lepton via b . This is strongly suppressed by the lepton isolation cut [10]. One also expects a fake LSD background from the direct leptonic decay of both t and \bar{t} , where one of the lepton charges is misidentified.

However, Ref. [9] did not take into account the effects of the top quark and Higgs bosons in the cascade decay process (1),(2), which are important for the resulting LSD signal. Inclusion of the top quark in the first step of the cascade decay gives [11, 12]

$$\tilde{g} \rightarrow \bar{t}b\chi_i^+ + \text{H.c.}, \quad (3)$$

$$\tilde{g} \rightarrow \bar{t}t\chi_i^0, \quad (4)$$

while that of Higgs bosons in the second step gives [12–14]

$$\chi_i^+ \rightarrow H^+\chi_1^0, \quad (5)$$

$$\chi_i^0 \rightarrow H_k^0\chi_1^0, \quad k = 1-3. \quad (6)$$

Both contributions have been studied earlier. But as far as we know, there is as yet no systematic analysis of their effects on the LSD signal at the LHC. The present work is devoted to this exercise. We shall estimate the

*Electronic address: dproy@theory.tifr.res.in

LSD signal arising from the cascade decay of a gluino at the LHC using a parton level Monte Carlo (MC) program as in [9], but including the top quark and Higgs boson effects. In the process we shall frequently draw upon the results of earlier works on top quark [11, 12] and Higgs boson [12–14] contributions to the cascade decay. Our emphasis will be on identifying the main contributors to the leptonic decay of a gluino over different regions of the SUSY parameters, which is essential for understanding the parametric dependence of the resulting LSD signal. It may be noted here that there is a third contribution to the cascade decay, which was not taken into account in [9] — i.e., the loop-induced decay

$$\tilde{g} \rightarrow g\chi_i^0. \quad (7)$$

We shall not consider it here either, since its contribution to \tilde{g} decay is very small ($\leq 5\%$) throughout the parameter space of interest [11, 15]. Large values of branching fractions for (7) reported in [1] (p. 627) are incorrect. It is worth pointing this out, so that others do not discover it the hard way as we did.

Since the Higgs bosons have negligible couplings to the e and μ channels, their inclusion in the cascade decay (5),(6) reduces the leptonic branching fraction of \tilde{g} . Indeed, we shall see below that this reduction factor can be quite large (~ 2) over a part of the parameter space. Fortunately this is more than offset by the inclusion of the top quark contribution (3),(4), which provides an extra source of $W \rightarrow \ell\nu$.

We have incorporated two other changes in this analysis in comparison with Ref. [9]. First, the recent Martin-Roberts-Stirling set D'_- (MRSD' $_-$) parametrization [16] for the gluon structure function has been used instead of Gluck, Hoffman, and Reya (GHR) [17]. It has a considerably steeper gluon, which results in a factor of ~ 2 reduction in the signal cross section from

$$gg \rightarrow \tilde{g}\tilde{g}, \quad (8)$$

over the gluino mass range of interest. We have also cross-checked this result with the Gluck-Reya-Vogt (GRV) parametrization [18], which is in good agreement with the MRSD' $_-$ [16]. Second, the c.m. energy has been reduced from 16 to 14 TeV, as currently projected for the LHC. This reduces the signal cross section by another fac-

tor of 2. Thus the updates of the gluon parametrization and the LHC energy reduce the signal cross section by a sizable factor of 4–5 [19]. Fortunately the LSD background from $t\bar{t}$ is also reduced by a similar factor, so that the signal/background ratio remains viable over most of the parameter space of interest. We have checked that our signal cross sections are consistent with those of Baer *et al.* [12] after taking account of this factor.

In the following section we briefly discuss the cascade decay process and identify the parameter space of interest. The gluino mass range of interest for the LHC can be divided into two parts: (i) the low mass region ($M_{\tilde{g}} \sim 300$ GeV) in which case the top quark contributions (3),(4) are kinematically forbidden or highly suppressed and (ii) the high mass region ($M_{\tilde{g}} \sim 800$ GeV) where top quark contributions (3),(4) are important. The relevant branching fractions for the cascade decay and the resulting LSD signals for these two cases are discussed in Secs. III and IV. The main results are summarized in Sec. V.

II. CASCADE DECAY PARAMETERS

The cascade decay formalism has been widely discussed in the literature [4–6, 20]. We shall only mention the essential points in order to fix the notation and identify the relevant parameters. We shall work within the framework of the minimal supersymmetric standard model (MSSM), which has the minimum number of parameters. We shall generally assume

$$M_{\tilde{g}} < M_{\tilde{q}}, \quad (9)$$

so that the gluino provides the most important signal for superparticle production at the LHC. With this assumption the gluino decay into chargino and neutralino states is insensitive to the squark mass. Our numerical results are obtained with a common squark mass $M_{\tilde{q}} = M_{\tilde{g}} + 200$ GeV.

There are four neutralino mass eigenstates, which are mixtures of the four interaction eigenstates: i.e.,

$$\chi_i^0 = N_{i1}\tilde{B} + N_{i2}\tilde{W}^3 + N_{i3}\tilde{H}_1^0 + N_{i4}\tilde{H}_2^0. \quad (10)$$

The masses and compositions of the neutralinos are obtained by diagonalizing the mass matrix

$$M_N = \begin{pmatrix} M_1 & 0 & -M_Z \sin \theta_W \cos \beta & M_Z \sin \theta_W \sin \beta \\ 0 & M_2 & M_Z \cos \theta_W \cos \beta & -H_Z \cos \theta_W \sin \beta \\ -M_Z \sin \theta_W \cos \beta & M_Z \cos \theta_W \cos \beta & 0 & -\mu \\ M_Z \sin \theta_W \sin \beta & -M_Z \cos \theta_W \sin \beta & \mu & 0 \end{pmatrix}, \quad (11)$$

where μ is the supersymmetric Higgsino mass parameter and $\tan \beta$ is the ratio of the two Higgs vacuum expectation values. M_1 and M_2 are the soft masses for B -ino \tilde{B} and W -ino \tilde{W} , respectively, which are related to the gluino mass in the MSSM: i.e.,

$$\begin{aligned} M_2 &= \frac{\alpha}{\sin^2 \theta_W \alpha_s} M_{\tilde{g}} \simeq 0.3 M_{\tilde{g}}, \\ M_1 &= \frac{5}{3} \tan^2 \theta_W M_2 \simeq 0.5 M_2. \end{aligned} \quad (12)$$

We have followed the analytical prescription of [21] for diagonalizing this mass matrix, but cross-checked our results with the numerical diagonalization program EISCH1.FOR as well as the published results of [1, 4, 22].

The chargino mass matrix

$$M_C = \begin{pmatrix} M_2 & \sqrt{2} M_W \sin \beta \\ \sqrt{2} M_W \cos \beta & \mu \end{pmatrix} \quad (13)$$

is diagonalized via the biunitary transformation

$$U M_c V^{-1} \quad (14)$$

to obtain the mass eigenvalues. The corresponding chargino eigenstates are

$$\begin{aligned} \chi_{iL}^\pm &= V_{i1} \tilde{W}_L^\pm + V_{i2} \tilde{H}_L^\pm, \\ \chi_{iR}^\pm &= U_{i1} \tilde{W}_R^\pm + U_{i2} \tilde{H}_R^\pm, \end{aligned} \quad (15)$$

where L and R refer to left and right chirality states. We shall use the real orthogonal representation of the unitary matrices U , V , and N . The chargino and neutralino states will be labeled in increasing order of mass, with χ_1^0 representing the LSP.

Thus the chargino and neutralino masses and compositions are specified in terms of the three parameters (i) $M_{\tilde{g}}$, (ii) μ , and (iii) $\tan\beta$, which in turn determine the cascade decay processes (1),(2).

(i) The gluino mass range of interest at the LHC is 200 GeV, to ~ 1 TeV. We shall choose two representative values

$$M_{\tilde{g}} = 300 \text{ and } 800 \text{ GeV}, \quad (16)$$

corresponding to a relatively light and heavy gluino. As we shall see below, the relevant cascade decay processes for the two cases are very different.

(ii) There are two distinct regions in the μ parameter space corresponding to $|\mu| > M_2$ and $|\mu| < M_2$. It is intuitively clear from (11) and (13) that the lighter chargino (χ_1^\pm) and neutralinos ($\chi_{1,2}^0$) are gaugino dominated in the former case and Higgsino dominated in the

latter. For the above range of $M_{\tilde{g}}$, the region

$$-40 \text{ GeV} \lesssim \mu \lesssim 80 \text{ GeV} \quad (17)$$

is excluded by the LEP data [22]. It corresponds to a Higgsino-dominated χ_1^0 with mass $< M_Z/2$, which would show up in Z decay. We shall take two pairs of values consistent with the LEP limits (17):

$$\mu = \pm 4M_W \text{ and } \pm M_W, \quad (18)$$

which represent the two regions mentioned above.

(iii) The results are rather insensitive to $\tan\beta$ over the range allowed by the MSSM:

$$1 < \tan\beta < m_t/m_b (\simeq 40), \quad (19)$$

except for some Higgs boson contributions as discussed below. We shall choose $\tan\beta = 2$ and 10 as two representative values. The current lower mass bounds of H_2^0 seems to disfavor $\tan\beta \simeq 1$ [see Eqs. (20) and (24) below], although it cannot be ruled out in view of the large radiative correction [23].

Inclusion of the top quark in the cascade decay (3),(4) requires the knowledge of m_t . We shall use the value $m_t = 175$ GeV, suggested by the recent Collider Detector at Fermilab (CDF) data [24]. Finally, the inclusion of Higgs bosons in the cascade decay (5),(6) brings in one more parameter, which can be taken as the charged Higgs boson mass. Then the neutral Higgs boson masses are given by the MSSM mass relation (at the tree level) [13, 20]

$$\begin{aligned} M_{H_3^0}^2 &= M_{H^\pm}^2 - M_W^2, \\ M_{H_1^0, H_2^0}^2 &= \frac{1}{2} \left[M_{H_3^0}^2 + M_Z^2 \pm \left\{ \left(M_{H_3^0}^2 + M_Z^2 \right)^2 - \left(2M_Z M_{H_3^0} \cos 2\beta \right)^2 \right\}^{\frac{1}{2}} \right], \end{aligned} \quad (20)$$

which imply

$$M_{H^\pm} > M_W (80 \text{ GeV}), \quad M_{H_2^0} < M_Z (91 \text{ GeV}). \quad (21)$$

We shall consider two extreme cases:

$$\begin{aligned} M_{H^\pm} = 500 &\implies M_{H_3^0} = 494, \quad M_{H_1^0} = 499(494), \quad M_{H_2^0} = 54(89), \\ M_{H^\pm} = 100 &\implies M_{H_3^0} = 60, \quad M_{H_1^0} = 104(92), \quad M_{H_2^0} = 31(58), \end{aligned} \quad (22)$$

for $\tan\beta = 2(10)$, where all the masses are in GeV. Thus, to a first approximation,

$$\begin{aligned} M_{H^\pm} \sim 500 \text{ GeV} &\implies M_{H_1^0}, \quad M_{H_3^0} \sim 500 \text{ GeV}, \quad M_{H_2^0} \lesssim 100 \text{ GeV}, \\ M_{H^\pm} \sim 100 \text{ GeV} &\implies M_{H_1^0}, \quad M_{H_3^0}, M_{H_2^0} \lesssim 100 \text{ GeV}, \end{aligned} \quad (23)$$

which will be adequate for our purpose. In the first case only H_2^0 will participate in the cascade decay while in the second case all the Higgs bosons will participate in it. The LEP mass limits for these Higgs bosons are [23]

$$M_{H^\pm} > 41.7 \text{ GeV}, \quad M_{H_3^0} > 22 \text{ GeV}, \quad M_{H_2^0} > 44 \text{ GeV}. \quad (24)$$

III. SIGNATURE FOR A LOW MASS GLUINO ($M_{\tilde{g}} = 300$ GeV)

In this case the top quark contributions (3),(4) are kinematically forbidden (or strongly suppressed). Thus

only the light quarks participate in the \tilde{g} decay into χ_i^\pm, χ_i^0 as shown in the first steps of (1),(2). Consequently one can neglect the interference terms between the right- and left-handed squark exchange amplitudes. More importantly one can also neglect the Yukawa couplings associated with the Higgsino components of χ_i^\pm and χ_i^0 , so that the \tilde{g} decay into these states is only governed by their gaugino components in (10),(15). The relevant decay amplitudes as well the compositions of the χ_i^\pm and χ_i^0 states can be found in [9]. We show the resulting branching fractions along with the χ_i^\pm and χ_i^0 masses in Table I for convenience. The dominant decay channels of the gluino are seen to be the lighter chargino (χ_1^\pm) and neutralino ($\chi_{1,2}^0$) states, which are gaugino dominated.

This is true not only at $\mu = \pm 4 M_W$, but remains approximately valid even at $\mu = -M_W$, which is close to the boundary of the allowed parameter space (17). The reason of course is that the condition $|\mu| > M_2 (\simeq 0.3 M_{\tilde{g}})$ holds practically throughout the allowed parameter space for $M_{\tilde{g}} \simeq 300$ GeV. Note that $\mu = M_W$ is already disallowed by the LEP data as indicated by the corresponding χ_1^0 and χ_1^\pm masses. It may be added here that the negative sign of some of the mass eigenvalues appearing in this

table will be relevant for their couplings and the resulting decay widths as discussed below [4, 13, 20].

Coming to the second step of the cascade decay, we see that the only decays of χ_1^\pm and χ_2^0 kinematically allowed are three-body decays into the LSP (χ_1^0) via virtual gauge (W, Z) or Higgs (H^\pm, H_k^0) bosons [25]. We shall give the formulas for the three-body decay widths since they are not readily available in the literature. They have been derived using the Feynman rules of [20]:

$$\begin{aligned} \Gamma_{\chi_i^\pm \rightarrow \chi_j^0 \bar{f} f'} &= \frac{9g^4}{(8\pi M_i)^3} \int ds \lambda^{\frac{1}{2}}(M_i^2, M_j^2, s) \left[\frac{1}{3} (G_L^2 + G_R^2) \left\{ (M_i^2 - M_j^2)^2 + s(M_i^2 + M_j^2 - 2s) \right\} - 4G_L G_R \epsilon_i \epsilon_j M_i M_j s \right], \\ G_L &= N_{j2} V_{i1} - \frac{1}{\sqrt{2}} N_{j4} V_{i2}, \\ G_R &= N_{j2} U_{i1} + \frac{1}{\sqrt{2}} N_{j3} U_{i2}, \end{aligned} \quad (25)$$

where ϵ_i, ϵ_j represent the signs of the χ_i^\pm, χ_j^0 masses and a sum over f and f' is understood. As usual,

$$\lambda(M_i^2, M_j^2, s) = (M_i^2 + M_j^2 - s)^2 - 4M_i^2 M_j^2, \quad (26)$$

$$\begin{aligned} \Gamma_{\chi_i^\pm \rightarrow \chi_j^\pm \bar{f} f'} &= \frac{g^4}{(8\pi M_i)^3} \frac{m_\tau^2 \tan^2 \beta}{2M_W^2} \int ds \lambda^{\frac{1}{2}}(M_i^2, M_j^2, s) \left[\frac{(F_L^2 + F_R^2)(M_i^2 + M_j^2 - s) + 4F_L F_R \epsilon_i \epsilon_j M_i M_j s}{(s - M_{H^\pm}^2)^2} \right], \\ F_L &= \cos \beta \left[N_{j4} V_{i1} + \frac{1}{\sqrt{2}} (N_{j2} + N_{j1} \tan \theta_W) V_{i2} \right], \\ F_R &= \sin \beta \left[N_{j\beta} U_{i1} - \frac{1}{\sqrt{2}} (N_{j2} + N_{j1} \tan \theta_W) U_{i2} \right], \end{aligned} \quad (27)$$

where the factor in front of the integral comes from H^\pm coupling to the $\tau\nu$ channel, which dominates its decay for $\tan \beta > 1$:

$$\begin{aligned} \Gamma_{\chi_i^0 \rightarrow \chi_j^0 \bar{f} f'} &= \frac{4g^4 \sum_f 2(g_V^{f2} + g_A^{f2}) G'^2}{\cos^4 \theta_W (8\pi M_i)^3} \int ds \lambda^{\frac{1}{2}}(M_i^2, M_j^2, s) \left[\frac{1}{3} \left\{ (M_i^2 - M_j^2)^2 + s(M_i^2 + M_j^2 - 2s) \right\} + 2\epsilon_i \epsilon_j M_i M_j s \right], \\ G' &= \frac{1}{2} (N_{i3} N_{j3} - N_{i4} N_{j4}), \\ \sum_f 2(g_V^{f2} + g_A^{f2}) &= \sum_f (T_3^{f2} - \sin^2 \theta_W T_3^f Q^f + 2 \sin^4 \theta_W Q_f^2) = 3.6, \end{aligned} \quad (28)$$

where the summation runs over all the leptons and quarks up to b , and $\sin^2 \theta_W = 0.23$ [23]:

$$\begin{aligned} \Gamma_{\chi_i^0 \rightarrow \chi_j^0 \bar{f} f'} &= \frac{3g^4 m_b^2 a_k^2 F_{ijk}^2}{M_W^2 \cos^2 \beta (8\pi M_i^3)} \int ds \lambda^{\frac{1}{2}}(M_i^2, M_j^2, s) \\ &\times \frac{\left[(M_i + \epsilon_i \epsilon_j \eta_k M_j)^2 - s \right] s}{(s - M_{H_k^0}^2)^2}, \\ F_{ijk} &= \frac{1}{2} e_k [N_{i3} N_{j2} + N_{j3} N_{i2} - \tan \theta_W \\ &\times (N_{i3} N_{j1} + N_{j3} N_{i1})] \\ &+ \frac{1}{2} f_k [N_{i4} N_{j2} + N_{j4} N_{i2} - \tan \theta_W \\ &\times (N_{i4} N_{j1} + N_{j4} N_{i1})], \\ \eta_{1,2,3} &= 1, 1, -1, \\ a_{1,2,3} &= \cos \alpha, \sin \alpha, \sin \beta, \\ e_{1,2,3} &= -\cos \alpha, \sin \alpha, \sin \beta, \\ f_{1,2,3} &= \sin \alpha, \cos \alpha, \cos \beta, \end{aligned} \quad (29)$$

where

$$\tan 2\alpha = \tan 2\beta \left(\frac{M_{H_1^0}^2 + M_{H_3^0}^2}{M_{H_3^0}^2 - M_Z^2} \right). \quad (30)$$

An alternative but equivalent expression for F_{ijk} is given in [13].

Let us compare the $\chi_1^\pm \rightarrow \chi_1^0$ decay widths via virtual W and H^\pm given in (25) and (27), respectively. The factors in front of the integrals came from the decay vertices of the virtual W and H^\pm bosons. The latter is relatively suppressed by a factor $\sim 3 \times 10^{-5} \tan^2 \beta$, which is $\ll 1$ throughout the $\tan \beta$ range (19) of interest. In addition, there is a larger propagator suppression factor for (27) relative to (25) in view of the mass inequality (21). The remaining factors are expected to be comparable, since $G_{L,R} \sim F_{L,R}$; they represent W and H^\pm couplings to $\chi_1^\pm \chi_1^0$ and are each suppressed by an off-diagonal element of the composition matrices. Thus one can safely neglect the Higgs boson contribution to the $\chi_1^\pm \rightarrow \chi_1^0$ decay. Hence the cascade decay

$$\tilde{g} \rightarrow \bar{q} q' \chi_1^\pm, \quad \chi_1^\pm \xrightarrow{1} W \chi_1^0 \xrightarrow{0.22} \ell \nu \chi_1^0 \quad (31)$$

is expected to provide a leptonic branching fraction of

$$0.22 B_{\tilde{g} \rightarrow \bar{q} q' \chi_1^\pm} \sim 0.1 \quad (32)$$

over most of the parameter space (see Table I) [26].

A similar comparison between the $\chi_2^0 \rightarrow \chi_1^0$ widths via (28) and (29) shows that the factors in front of the in-

tegrals, coming from the decay vertices of the virtual Z and H_k^0 , are already comparable for $\tan\beta = 10$. Moreover, the $\chi_2^0\chi_1^0$ coupling of Z is smaller than those of H_k^0 —i.e., $G' < F_{21k}$. That is because G' is suppressed by two off-diagonal elements of the composition matrix, since Z couples to a pair of neutralinos only through their Higgsino components. Finally the propagator suppression for Z is larger than that of H_2^0 because of (21). Thus the virtual Higgs contribution to the $\chi_2^0 \rightarrow \chi_1^0$ decay is expected to dominate over the Z contribution for $\tan\beta \geq 10$. Hence the leptonic decay mode of \tilde{g} via χ_2^0 ,

$$\tilde{g} \rightarrow \bar{q}q\chi_2^0, \quad \chi_2^0 \rightarrow Z\chi_1^0 \xrightarrow{0.06} \ell^+\ell^-\chi_1^0, \quad (33)$$

is suppressed over a large part of the parameter space.

TABLE I. Masses (in GeV) and gluonic branching fractions of the two chargino $\chi_{1,2}^\pm$ and four neutralino χ_{1-4}^0 states for $M_{\tilde{g}} = 300$ GeV.

$\tan\beta$	μ	$M_{\chi_i^\pm}$	$B_{\tilde{g} \rightarrow \bar{q}q'\chi_i^\pm}$	$M_{\chi_i^0}$	$B_{\tilde{g} \rightarrow \bar{q}q\chi_i^0}$	
2	$4M_W$	77.7	0.47	42.3	0.20	
		349.8	0	81.8	0.32	
				-326.4	0	
				352.9	0	
	$-4M_W$	110.6	0.47	53.6	0.20	
				110.7	0.32	
2	340.8	0	328.0	0		
				-341.9	0	
$-M_W$	91.5	0.30	54.9	0.20		
				73.1	0.11	
			146.2	0.19	-118.4	0.04
				141.3	0.16	
	M_W	16.6		-0.1	63.3	
		171.6		-87.5	175.0	
10	$4M_W$	89.8	0.52	48.2	0.17	
		346.9	0	90.6	0.31	
				-332.5	0	
				344.3	0	
	$-4M_W$	97.9	0.50	50.9	0.18	
				97.8	0.31	
10	344.7	0	-336.3	0		
				338.2	0	
$-M_W$	58.0	0.42	37.2	0.15		
				65.0	0.22	
			162.4	0.10	-109.0	0.04
				157.5	0.08	
M_W	40.6		23.3			
				63.9		
	167.6		-101.8			
			165.3			

We shall neglect this mode altogether in estimating the LSD signal below. It may be added here that, without the Higgs contribution, this process would effectively add $\sim 40\%$ to the leptonic branching fraction of (31),(32) and hence double the resulting LSD signal [9]. Of course its contribution to the LSD signal comes from the three- and four-lepton final states, while the exclusive LSD state comes only from the decay mode (31) of the gluino pair.

Figure 1 shows the isolated LSD signal from (31) against the p_T of the softer lepton for $\mu = \pm 4M_W$ and $-M_W$. In the last case there is also a modest contribution via the χ_2^\pm state. An isolation cut of

$$E_T^{\text{ac}} < 10 \text{ GeV} \quad (34)$$

has been applied on both the leptons, where E_T^{ac} is the transverse energy accompanying a lepton within a cone of $\Delta R = (\Delta\phi^2 + \Delta\eta^2)^{1/2} = 0.4$. A nominal rapidity cut of $|n_\ell| < 3$ has also been applied to the leptons. The signal is seen to be remarkably insensitive to the choice of μ as well as $\tan\beta$. As per (31),(32) about 1% of the gluino pair decays into a dilepton final state, so that the LSD signal occurs at the level of $\sim 1/2\%$ of the $\tilde{g}\tilde{g}$ cross section.

Figure 1 also shows the two backgrounds from $t\bar{t}$ production mentioned above — i.e., the LSD background from

$$t \rightarrow b\ell^+\nu, \quad \bar{t} \rightarrow \bar{b} \rightarrow \bar{c}\ell^+\nu, \quad (35)$$

as well as a fake LSD background from

$$t \rightarrow b\ell^+\nu, \quad \bar{t} \rightarrow \bar{b}\ell^-\bar{\nu}, \quad (36)$$

where one of the lepton charges is misidentified. The fake LSD background has been set at the level of 1% of the cross section for (36), corresponding to a conserva-

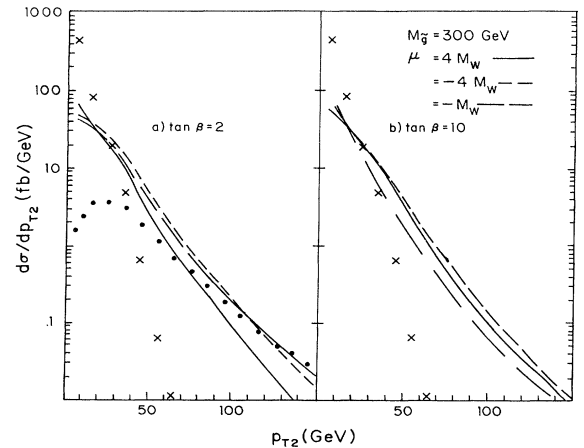


FIG. 1. The LSD signals for 300 GeV gluino production at LHC shown against the p_T of the second (softer) lepton for $\mu = \pm 4M_W$, $-M_W$, and $\tan\beta = 2, 10$. Also shown are the LSD backgrounds from $t\bar{t}$ production — a real background arising from the leptonic decay of one t via b (crosses) and a fake background arising from the misidentification of one of the lepton charges (dots), which is conservatively assumed to be 1% of the dilepton cross section (36).

tive estimate of 1/2% probability for misidentification of one of the lepton charges. The isolation cut effectively suppresses the LSD background (35) for $p_{T_2} \gtrsim 50$ GeV [10], but not the fake background from (36). However, there is a large amount of missing p_T accompanying the LSD signal, thanks to the ν and χ_1^0 in (31). This can be exploited to separate the signal from the backgrounds, as we shall see later in Fig. 4 [27].

IV. SIGNATURE FOR A HIGH MASS GLUINO ($M_{\tilde{g}} = 800$ GeV)

In this case one has to include the top quark contributions (3),(4) along with the light quark contributions to gluino decay shown in the first steps of (1),(2). The latter contributions are calculated in the same way as before. The results are also very similar except for one case. At $\mu = -M_W$, the magnitude of μ is now significantly lower than M_2 , so that the lighter chargino and neutralino states are Higgsino dominated. Consequently the gluino decays preferentially into the heavier chargino (χ_2^\pm) and neutralino ($\chi_{3,4}^0$) states, which are gaugino dominated. The branching fractions are shown in Table II for $\mu = -M_W$ and $4M_W$. The results for

$\mu = -4M_W$ are similar to those of $4M_W$ and hence not shown. Instead we include the point $\mu = 6M_W$, which will be relevant for the top quark contributions discussed below.

For the gluino decay processes (3),(4) involving the top quark one has to include the interference terms between the right- and left-handed squark exchanges as well as the Yukawa couplings associated with the Higgsino components of χ_i^\pm and χ_i^0 . Consequently the squared matrix elements for (3) and (4) are very long. These are given in Ref. [11]. We have used them in calculating the decay rates for (3) and (4). The resulting branching fractions are shown in Table II.

Here the Higgsino components of χ_i^\pm and χ_i^0 play a very important role in determining the gluino branching fractions. At $\mu = -M_W$, where the Higgsino-dominated states χ_1^\pm and $\chi_{1,2}^0$ are kinematically favored, they account for the largest branching fractions of the gluino unlike the light quark contribution. At $\mu = 4M_W$, the Higgsino-dominated states χ_2^\pm and $\chi_{3,4}^0$ have an equal share of the branching fractions in spite of being kinematically disfavored. Only at $\mu = 6M_W$, do these Higgsino-dominated states become kinematically inaccessible, so that the gluino decays only into the gaugino-dominated ones. It is interesting to note that the net top quark

TABLE II. Masses (in GeV) and gluonic branching fractions of two chargino $\chi_{1,2}^\pm$ and four neutralino χ_{1-4}^0 states for $M_{\tilde{g}} = 800$ GeV.

$\tan\beta$	μ	$M_{\chi_i^\pm}$	$B_{\tilde{g} \rightarrow \bar{q}q' \chi_i^\pm}$	$B_{\tilde{g} \rightarrow \bar{t}b \chi_i^+ + hc}$	$M_{\chi_i^0}$	$B_{\tilde{g} \rightarrow \bar{q}q \chi_i^0}$	$B_{\tilde{g} \rightarrow \bar{t}t \chi_i^0}$		
	$-M_W$	92	0.02	0.32	75	0	0.11		
					-103	0	0.11		
		286	0.14	0.11	143	0.05	0.04		
					286	0.07	0.03		
	2	$4M_W$	213	0.24	0.15	124	0.11	0.02	
						220	0.14	0.03	
375			0.04	0.17	-321	0	0.04		
					378	0.02	0.04		
$6M_W$		243	0.39	0.16	127	0.15	0.03		
						244	0.24	0.02	
	505		0	0	-481	0	0		
					508	0	0		
		$-M_W$	78	0.04	0.28	61	0.02	0.08	
						-96	0.01	0.12	
291			0.12	13	146	0.05	0.04		
						290	0.08	0.03	
10			$4M_W$	229	0.25	0.12	130	0.11	0.02
							232	0.15	0.02
		366		0.04	0.18	-326	0	0.03	
						365	0.02	0.05	
		$6M_W$	253	0.37	0.17	131	0.16	0.03	
							256	0.24	0.02
500			0	0	-485	0	0		
					496	0	0		

contribution to the gluino decay is as large as 70% at $\mu = -M_W$, going down to 40% at $4M_W$ and 20% at $6M_W$. The last value holds for the $\mu > 6M_W$ region as well. Its excess share at lower values of μ arises from the Yukawa couplings of charginos and neutralinos associated with the large top quark mass. It is important for the resulting LSD signal as we shall see below.

We shall be interested in the leptonic branching fractions of the top quark,

$$t \xrightarrow{1} bW \xrightarrow{0.22} b\nu, \quad (37)$$

as well as the chargino and neutralino states of Table II. Clearly

$$\chi_1^\pm \xrightarrow{1} W\chi_1^0 \xrightarrow{0.22} \ell\nu\chi_1^0, \quad (38)$$

whether the W is real or virtual, since the competing H^\pm will be always virtual and hence suppressed for the reasons discussed earlier. For the same reason we expect

$$\chi_2^\pm \rightarrow \chi_1^0 W, \chi_1^0 H^\pm, \chi_2^0 W, \chi_2^0 H^\pm, \chi_1^\pm Z, \chi_1^\pm H_1^0, \chi_1^\pm H_2^0, \chi_1^\pm H_3^0 \quad (40)$$

are $\tan^2 \theta_W (\simeq 1/3)$ for the first two and 1 for the rest. Recall from (23) that all the five Higgs channels are kinematically accessible for $M_{H^\pm} \sim 100$ GeV, while only the H_2^0 channel is accessible for $M_{H^\pm} \sim 500$ GeV. Consequently one has the following branching fractions for χ_2^\pm for $M_{H^\pm} \sim 500(100)$ GeV:

$$\begin{aligned} \chi_2^\pm &\xrightarrow{0.1(0.05)} \chi_1^0 W \xrightarrow{0.22} \chi_1^0 \ell\nu, \\ \chi_2^\pm &\xrightarrow{0.3(0.15)} \chi_2^0 W \xrightarrow{0.22} \chi_2^0 \ell\nu, \\ \chi_2^\pm &\xrightarrow{0.3(0.15)} \chi_1^\pm Z \xrightarrow{0.06} \chi_1^\pm \ell^+ \ell^-. \end{aligned} \quad (41)$$

For $|\mu| < M_{1,2}$, corresponding to the point $\mu = -M_W$, the relative branching fractions of all the channels in (40) are equal. Consequently one gets

$$\begin{aligned} \chi_2^\pm &\xrightarrow{0.25(0.12)} \chi_1^0 W \xrightarrow{0.22} \chi_1^0 \ell\nu, \\ \chi_2^\pm &\xrightarrow{0.25(0.12)} \chi_2^0 W \xrightarrow{0.22} \chi_2^0 \ell\nu, \\ \chi_2^\pm &\xrightarrow{0.25(0.12)} \chi_1^\pm Z \xrightarrow{0.06} \chi_1^\pm \ell^+ \ell^-, \end{aligned} \quad (42)$$

for $M_{H^\pm} \sim 500(100)$ GeV. We shall not consider the lepton from the χ_1^\pm decay in the last line as it would be further degraded in p_T .

The LSD signal comes from the leptonic decay of each gluino arising from any of the above processes. For $\mu = -M_W$, the major contributions are from

$$\tilde{g} \rightarrow \bar{q}q'\chi_2^\pm, \quad \bar{t}b\chi_1^+ + \text{H.c.}, \quad \bar{t}b\chi_2^+ + \text{H.c.}, \quad \bar{t}t\chi_1^0, \quad (43)$$

followed by the leptonic decays of (37), (38), or (42). The LSD signal so calculated includes the contributions from the three- and four-lepton states, but the size of these contributions is relatively small. The three-lepton contribution accounts for a little under a quarter of the signal while the four-lepton contribution is negligible. The resulting LSD signal is shown in Fig. 2 for $\tan\beta = 2$ and 10. In each case the signal is shown for the two extreme choices of $M_{H^\pm} = 500$ and 100 GeV. It is seen to be

the

$$\chi_2^0 \rightarrow H_2^0 \chi_1^0 \quad (39)$$

to dominate over a large part of the parameter space and hence not be of interest for the leptonic decay.

We have to also consider the leptonic decays of the heavier chargino and neutralino states here. It is clear from their masses that they undergo two-body decay emitting real W , Z , or Higgs bosons. These two-body decays have been widely discussed in the literature [12–14]. The $\chi_{3,4}^0$ decays are Higgs boson dominated over large parts of the parameter spaces, and besides their contributions to gluino decay are relatively small. Therefore we shall concentrate on the χ_2^\pm decay. Moreover, we shall use the asymptotic values of its branching fractions given in [13], for large $M_{1,2}$ or $|\mu|$, since they are simple and accurate enough for our purpose. For $|\mu| > M_{1,2}$, which holds for the point $\mu = 4M_W$, the relative branching fractions of χ_2^\pm into the channels

insensitive to either of these parameters. Note that the light quark contribution to the leptonic branching fraction of the gluino comes mainly from the χ_2^\pm decay (42), where the reduction factor from the Higgs boson effect can be as large as 3/8. This is more than offset, however, by the top quark contribution so that the net LSD signal is large as well as insensitive to the Higgs boson effect. The size of the LSD signal is at the level of $\sim 4\%$ of the $\tilde{g}\tilde{g}$ cross section i.e., an order of magnitude larger than the case discussed earlier. The major part of this signal comes from the leptonic decay of the gluino pair via the top quark. It is a characteristic feature of the Majorana nature of the gluino, however, that the pair of top quarks and the resulting leptons have like charge half the time. For $\mu = 4M_W$, the major contributions are from

$$\tilde{g} \rightarrow \bar{q}q'\chi_1^\pm, \quad \bar{t}b\chi_1^+ + \text{H.c.}, \quad \bar{t}b\chi_2^+ + \text{H.c.}, \quad (44)$$

followed by the leptonic decays of (37), (38), or (41). The corresponding LSD signal is shown in Fig. 3. The size of this signal is a little less than half of that for $\mu = -M_W$. The reason of course is the reduced top quark contribu-

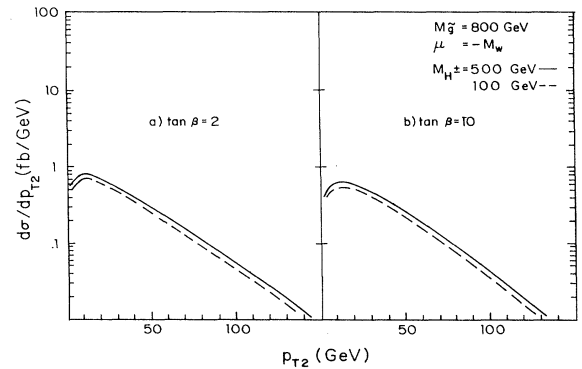


FIG. 2. The LSD signals for 800 GeV gluino production at LHC for $\mu = -M_W$, $M_{H^\pm} = 500, 100$ GeV, and $\tan\beta = 2, 10$.

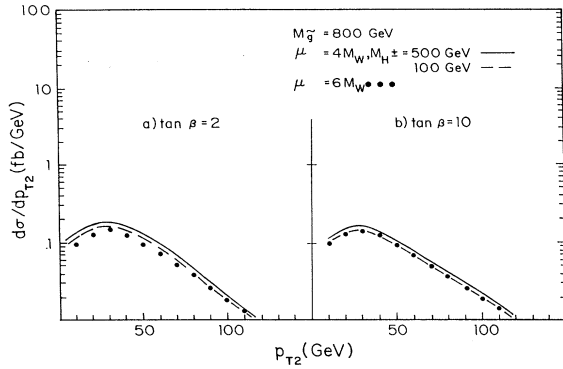


FIG. 3. The LSD signals for 800 GeV gluino production at LHC for $\mu = 4M_W$, $M_{H^\pm} = 500, 100$ GeV, and $\tan\beta = 2, 10$. Also shown are the signals for $\mu = 6M_W$ which are practically independent of M_{H^\pm} .

tion to gluino decay, as remarked earlier. Figure 3 also shows the signal for $\mu = 6M_W$. In this case the last channel of (44) is kinematically forbidden. Consequently there is no dependence on the charged Higgs boson mass. There is only a slight reduction in the signal in going from $\mu = 4M_W$ to $6M_W$. The signal is expected to remain at this level for higher values of μ as well.

The LSD signals for the 800 GeV gluino, shown in Figs. 2 and 3, can be separated from the LSD background of (35), shown in Fig. 1, by a $p_{T2} > 50$ GeV cut. But they remain below the level of the fake LSD background from (36). However, they can be distinguished by the amount of missing p_T accompanying the LSD events. Figure 4 shows the LSD signals for 300 and 800 GeV gluinos along with both the backgrounds against the accompanying missing p_T . A p_T cut of 20 GeV has been applied to both the leptons. There is a significantly larger amount of missing p_T accompanying the LSD signal compared to either background. The reason of course is that the signal events are accompanied by a pair of LSP's in addition to the neutrinos, as remarked earlier. Figure 4 shows the LSD signals, only for $\mu = 4M_W$, since the corresponding signals for $\mu = -M_W$ are very similar for $M_{\tilde{g}} = 300$ GeV and larger for $M_{\tilde{g}} = 800$ GeV.

Finally, Fig. 4 shows that the LSD signal for both the gluino masses can be separated from the backgrounds by an accompanying missing- p_T cut that retains about half the signal size. For a 800 GeV gluino, the size of the surviving signal is ~ 5 fb, corresponding to ~ 50 events per year for the typical low luminosity (~ 10 fb/y) option of the LHC. Thus one expects a viable LSD signal for a 800 GeV gluino over practically the full parameter space of the MSSM even at the low luminosity option of the LHC. The signal goes down by a factor of 3–4 for $M_{\tilde{g}} = 1000$ GeV and ~ 10 for $M_{\tilde{g}} = 1200$ GeV. Thus the LSD signal is expected to remain viable up to a gluino mass of 1200 GeV at the high luminosity option of the LHC, with an expected luminosity of ~ 100 fb/yr.

V. SUMMARY

We have undertaken a systematic analysis of the LSD signature for gluino production at the LHC in the

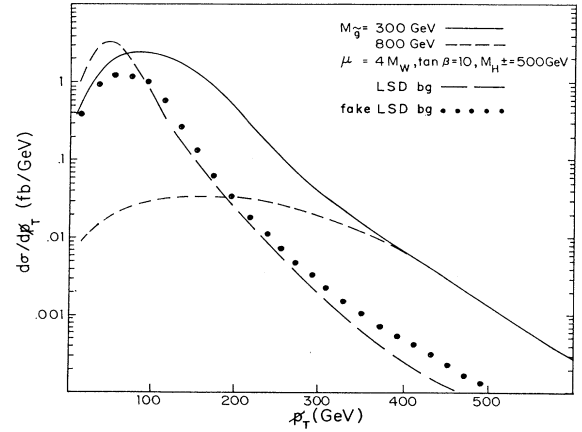


FIG. 4. The accompanying missing- p_T ($-p_T$) distribution of the LSD signals for 300 and 800 GeV gluino production at LHC for $\mu = 4M_W$, $\tan\beta = 10$, and $M_{H^\pm} = 500$ GeV. The real and fake LSD backgrounds from $t\bar{t}$ production are shown by long-dashed and dotted lines, respectively.

R -conserving minimal supersymmetric standard model, taking into account the top quark and Higgs boson effects in the cascade decay. We have considered two representative values of the gluino mass, 300 and 800 GeV, along with those of the other SUSY parameters, μ , $\tan\beta$, and M_{H^\pm} . The top quark mass has been taken to be 175 GeV, as suggested by the recent CDF data [24]. The main results are summarized below.

For a relatively low gluino mass of ~ 300 GeV, the top quark contribution is kinematically suppressed. Here the main contribution to the LSD signal comes from the three-body decay of the lighter chargino (χ_1^\pm) into the LSP (χ_1^0) via a virtual W boson. The signal is seen to be insensitive to μ and $\tan\beta$ as well as M_{H^\pm} . For a large gluino mass of ~ 800 GeV, the top quark contribution to the LSD signal is very important, particularly at small μ . Consequently one gets the largest signal at small μ , but it remains viable at larger values of μ as well. It is insensitive to the other parameters. A suitable cut on the accompanying missing p_T can separate the gluino signal from the underlying LSD background, while retaining about half the signal size. Even in the unfavorable case of large μ , the size of the surviving signal for an 800 GeV gluino is ~ 5 fb. This corresponds to ~ 50 events for the low luminosity option of the LHC. Thus the LSD signal provides an unambiguous signature for gluino production up to ~ 800 GeV at the low luminosity option of the LHC. At the high luminosity option the signature remains viable up to a gluino mass of ~ 1200 GeV.

ACKNOWLEDGMENTS

We are grateful to the organizers of WHEPP-3 at Madras, where this investigation was started as a working group project. We are also grateful to our colleagues from far and near, Mike Bisset, Manuel Drees, Rohini Godbole, N.K. Mondal, P.N. Pandita, Probir Roy, and Xerxes Tata for discussions. One of us (M.G.) acknowledges financial support from the Council of Scientific and Industrial Research, India.

- [1] Supersymmetry Working Group, C. Albajar *et al.*, in *Proceedings of the ECFA Large Hadron Collider Workshop*, Aachen, Germany, 1990, edited by G. Jarlskog and D. Rein (CERN Report No. 90-10, Geneva, Switzerland, 1990), Vol. II, pp. 606–683.
- [2] For a review see, e.g., H. Haber and G. Kane, *Phys. Rep.* **117**, 75 (1985).
- [3] J. Ellis, J. Hagelin, D. Nanopoulos, K. Olive, and M. Srednicki, *Nucl. Phys.* **B238**, 453 (1984).
- [4] H. Baer, V. Barger, D. Karatas, and X. Tata, *Phys. Rev. D* **36**, 96 (1987).
- [5] M. Barnett, J. Gunion, and H. Haber, *Phys. Rev. D* **37**, 1892 (1988); in *High Energy Physics in the 1990's*, Proceedings of the Summer Study on High Energy Physics, Snowmass, Colorado, 1988, edited by S. Jensen (World Scientific, Singapore, 1989), p. 230; in *Research Directions for the Decade*, Proceedings of the Summer Study on High Energy Physics, Snowmass, Colorado 1990, edited by E.L. Berger (World Scientific, Singapore, 1992), p. 201; *Phys. Lett. B* **315**, 349 (1993).
- [6] H. Baer, X. Tata, and J. Woodside, *Phys. Rev. D* **41**, 906 (1990).
- [7] H. Baer, C. Kao, and X. Tata, *Phys. Rev. D* **48**, R2978 (1993).
- [8] D.P. Roy, *Phys. Lett. B* **196**, 395 (1987).
- [9] H. Dreiner, M. Guchait, and D.P. Roy, *Phys. Rev. D* **49**, 3270 (1994).
- [10] N.K. Mondal and D.P. Roy, *Phys. Rev. D* **49**, 183 (1994).
- [11] A. Bartl, W. Majerotto, B. Mosslacher, N. Oshimo, and S. Stippel, *Phys. Rev. D* **43**, 2214 (1991).
- [12] H. Baer, X. Tata, and J. Woodside, *Phys. Rev. D* **45**, 142 (1992); H. Baer, M. Bisset, X. Tata, and J. Woodside, *ibid.* **46**, 303 (1992); A. Bartl, W. Majerotto, B. Mosslacher, and N. Oshimo, *Z. Phys. C* **52**, 477 (1991).
- [13] J. Gunion and H. Haber, *Phys. Rev. D* **37**, 2515 (1988).
- [14] H. Baer, A. Bartl, D. Karatas, W. Majerotto, and X. Tata, *Int. J. Mod. Phys. A* **4**, 4111 (1989).
- [15] H. Baer, X. Tata, and J. Woodside, *Phys. Rev. D* **42**, 1568 (1990).
- [16] A.D. Martin, R.G. Roberts, and W.J. Stirling, *Phys. Lett. B* **306**, 145 (1993); **309**, 492 (1993).
- [17] M. Gluck, E. Hoffman, and E. Reya, *Z. Phys. C* **13**, 119 (1982).
- [18] M. Gluck, E. Reya, and A. Vogt, *Z. Phys. C* **48**, 471 (1990); *Phys. Lett. B* **306**, 391 (1993).
- [19] This also applied to the LSD signal of [9] for the R -violating SUSY model, while the top quark and Higgs boson effects are insignificant in this case.
- [20] J. Gunion and H. Haber, *Nucl. Phys.* **B272**, 1 (1986).
- [21] M. Guchait, *Z. Phys. C* **57**, 157 (1993).
- [22] L. Roszkowski, *Phys. Lett. B* **262**, 59 (1991).
- [23] Particle Data Group, L. Montanet *et al.*, *Phys. Rev. D* **50**, 1173 (1994).
- [24] CDF Collaboration, F. Abe *et al.*, *Phys. Rev. Lett.* **73**, 225 (1994); *Phys. Rev. D* **50**, 2966 (1994).
- [25] Although there are marginal regions of the parameter space for which $\chi_2^0 \rightarrow \chi_1^0 H_{2,3}^0$ two-body decays are not yet strictly ruled out.
- [26] There is, however, a small region of the parameter space, corresponding to a small $M_{H^\pm} (\sim 100 \text{ GeV})$ and large $\tan \beta (\gtrsim 40)$ as well as $|\mu| (\gtrsim 500 \text{ GeV})$, where the H^\pm -mediated decay (27) may dominate over the W -mediated decay (25). The first two conditions ensure that the suppressions from the H^\pm propagator and decay vertex are not very large. Moreover, the last two conditions imply $G_{L,R} \ll F_{L,R}$, since $N_{12} \ll N_{13,14}$ and $U_{12} \ll U_{11} (V_{12} \ll V_{11})$ in this region [13]. Consequently there may not be a viable LSD signal in this corner of the parameter space.
- [27] There is also a LSD background from $b\bar{b}$ via missing p_T . But it is strongly suppressed by the isolation cut on the leptons [10]. Moreover, there is very little missing p_T accompanying this background. Several other sources of the LSD background have been discussed by Baer *et al.* [12].